AIAA 81-1875R

The Unsteady Suction Analogy and Applications

C. Edward Lan*
The University of Kansas, Lawrence, Kansas

A method of the unsteady suction analogy is developed by using the unsteady quasi-vortex-lattice method, which is capable of accurately predicting unsteady leading- and side-edge suction forces. The method is applicable to any reduced frequency. The importance of vortex lag is demonstrated. Good agreement in variation of predicted roll damping derivatives with reduced frequencies and angles of attack with data is shown. Applications to predicting longitudinal dynamic stability derivatives for slender wings at high angles of attack are presented.

Nomenclature

A = aspect ratio
b = span
$C(k)$ = Theodorsen's circulation function
$\bar{c}$ = mean aerodynamic chord
C_{ℓ_p} = $\partial C_\ell/\partial(pb/2V)$, roll damping derivative based on body axes
C_m = pitching moment coefficient
$C_{m_{\dot{\alpha}}}$ = $\partial C_m/\partial(\dot{\alpha}\ell_r/V)$
$C_{m_{\dot{h}}}$ = $\partial C_m/\partial(\omega h/V)$
C_{m_q} = $\partial C_m/\partial(q\bar{c}/2V)$, steady pitch damping derivative
C_{m_θ} = $\partial C_m/\partial\theta$
$C_{m_{\dot{\theta}}}$ = $\partial C_m/\partial(\theta\omega\ell_r/V)$
C_N = normal force coefficient
$C_{N_{\dot{h}}}$ = $\partial C_N/\partial(\omega h/V)$
ΔC_p = lifting pressure coefficient
c_r = root chord
C_Q = total leading-edge singularity parameter
c_s = sectional leading-edge suction coefficient
c_t = sectional leading-edge thrust coefficient
C_u = unsteady leading-edge singularity parameter
d = total leading-edge length
h = plunging amplitude
k = $\omega\ell_r/V$, reduced frequency
ℓ = leading-edge length along which a disturbance traverses
$\bar{\ell}$ = mean traversing distance of disturbance used in the definition of lumped phase angle
ℓ_c = characteristic length defined in Eq. (38)
ℓ_r = reference length
M = Mach number
N_c = number of chordwise discrete elements of doublets, or pressure modes
N_s = number of spanwise strips of doublet distribution, or collocation stations
p = roll rate
q = pitch rate
r = yaw rate
T = oscillation period
V = freestream velocity
w = normal wash
x,y,z = rectangular coordinate system defined in Fig. 1
x_a = x coordinate of pitching axis
z_c = camber ordinate
α,α_s = steady angle of attack
$\Delta\alpha$ = incremental angle of attack due to unsteady motion
β = $(1-M^2)^{1/2}$
Λ = leading-edge sweep angle
λ = taper ratio
ω = oscillation frequency
$\bar{\phi}$ = unsteady velocity potential
ϕ = velocity potential amplitude, or phase lag angle
ϕ_θ = amplitude of roll oscillation
$\bar{\phi}_r$ = unsteady roll angle
θ = pitching amplitude or integration variable
ξ,η,ζ = rectangular coordinates of elemental doublets

Subscripts

eff = effective
ℓ = leading edge
s = steady
t = trailing edge
u = unsteady

Presented as Paper 81-1875 at the AIAA Atmospheric Flight Mechanics Conference, Albuquerque, N. Mex., Aug. 19-21, 1981; submitted Oct. 5, 1981; revision received March 10, 1982.

*Professor of Aerospace Engineering. Associate Fellow AIAA.

Introduction

EDGE-separated vortex flow plays an important role in unsteady aerodynamic characteristics of slender wings.[1] Early attempts to solve the problem employed the slender wing theory with Smith's flow model.[2] More recently, a modified slender wing theory was used to calculate some longitudinal dynamic stability derivatives.[3,4] The unsteady vortex effects were accounted for by combining the experimental static pressure data with the vortex lag concept.[5] The method is applicable only at low reduced frequencies. Although the unsteady incompressible lifting-surface method with vortex flow is available,[6] its application to predicting dynamic stability derivatives at high angles of attack has not been demonstrated and the computing time is expected to be lengthy.

Applications of the unsteady aerodynamic theory to the prediction of dynamic stability derivatives of missile configurations have recently been reviewed by Schneider.[7] The assumption of very low frequency is usually made to simplify the formulation.

In this paper, an unsteady lifting-surface theory capable of accurately predicting unsteady leading- and side-edge suction forces will be used to develop a method of the unsteady suction analogy. The method will be applicable to any reduced frequency. Variation of roll damping derivatives with reduced frequencies and angles of attack will be compared with data. Applications to predicting longitudinal dynamic stability derivatives for slender wings at high angles of attack will be demonstrated.

Theoretical Development

Polhamus' method of suction analogy in steady flow[8] is based on the assumption that the vortex lift effect in a vortex-

separated flow can be predicted by utilizing the edge suction forces calculated in the attached flow theory. The attached flow theory used in the present method is the unsteady quasi-vortex-lattice method (unsteady QVLM) reported in Ref. 9. This method can accurately predict unsteady leading- and side-edge suction forces in the attached flow. The formulation given in Ref. 9 is mainly for the incompressible flow. Some preliminary three-dimensional results in subsonic flow have been reported in Ref. 10. In the following, the formulation of the compressible unsteady QVLM will be summarized. The extension of the steady suction analogy method to the unsteady case will then be described.

The Unsteady QVLM

The formulation is based on the linear compressible flow theory, with the coordinate system being defined in Fig. 1. The effect of wing thickness will not be included.

For a wing in plunging motion with displacement $\bar{h}(y,t)$, in pitching with angular displacement $\bar{\theta}(y,t)$ about $x=x_a$, and in rolling oscillation with roll angle $\bar{\phi}_r(t)$, the total vertical displacement $z(x,y,t)$ is given by

$$z(x,y,t) = -\bar{h}(y,t) - \bar{\theta}(y,t)\,(x-x_a) - y\bar{\phi}_r(t) \tag{1a}$$

It follows that the nondimensional normal wash on the wing is

$$\bar{w}(x,y,t) = \frac{1}{V}\frac{\partial z}{\partial t} + \frac{\partial z}{\partial x} = -\frac{\dot{\bar{h}}}{V} - \bar{\theta} - \frac{\dot{\bar{\theta}}}{V}(x-x_a) - \frac{y}{V}\dot{\bar{\phi}}_r(t) \tag{1b}$$

where V is the freestream velocity. Assuming the harmonic time variation such that $\bar{w}(x,y,t) = Re[w(x,y)\exp(i\omega t)]$, etc., Eq. (1b) becomes

$$-w(x,y) = \Delta\alpha = i\frac{k}{\ell_r}h(y) + \theta(y) + i\frac{k}{\ell_r}\theta(y)\,(x-x_a) + ik\frac{y}{\ell_r}\phi_0 \tag{2}$$

where $k=\omega\ell_r/V$ is the reduced frequency, ℓ_r the reference length, and ϕ_0 the roll angle amplitude. This additional angle of attack ($\Delta\alpha$) is added to the steady angle of attack (α_s) to produce the total normal wash (w_1) on the wing equal to

$$w_1(x,y) = \frac{\partial z_c}{\partial x}\cos\alpha_s - \sin(\alpha_s+\Delta\alpha) \cong \frac{\partial z_c}{\partial x}\cos\alpha_s - \sin\alpha_s - \Delta\alpha\cos\alpha_s \tag{3}$$

This total normal wash can be cancelled on the wing (i.e., satisfying the wing flow tangency condition) by the use of vortex distribution for the first two terms on the right side of Eq. (3),[11] and by the use of oscillating doublets for the last term. Considering now only the unsteady part, it was Richardson[12] who showed that the nondimensional velocity potential for doublets in an unsteady subsonic flow with Mach number M is given by

$$\bar{\phi}(x,y,z,t) = \frac{1}{8\pi}\iint_S \frac{\partial}{\partial\zeta}\int_{(-x_0+MR)/\beta^2}^{\infty} \Delta\bar{C}_p \times \left(\xi,\eta,t-\frac{\tau_1+x_0}{V}\right)\frac{1}{r}\,d\tau_1\,d\xi\,d\eta \tag{4}$$

where S is the wing area, $\Delta\bar{C}_p$ is the nondimensional lifting pressure, $\beta^2=1-M^2$, $x_0=x-\xi$, $y_0=y-\eta$, $z_0=z-\zeta$, (ξ,η,ζ) being the coordinates of an elemental doublet, and

$$r=(\tau_1^2+y_0^2+z_0^2)^{1/2} \tag{5}$$

$$R^2=x_0^2+\beta^2(y_0^2+z_0^2) \tag{6}$$

If the harmonic time variation is introduced, then

$$\bar{\phi}(x,y,z,t) = \phi(x,y,z)\exp(i\omega t) \tag{7}$$

$$\Delta\bar{C}_p\left(\xi,\eta,t-\frac{\tau_1+x_0}{V}\right) = \Delta C_{pu}(\xi,\eta)\exp(i\omega t)\exp[-i\omega(\tau_1+x_0)/V] \tag{8}$$

Hence, Eq. (4) is reduced to

$$\phi(x,y,z) = \frac{1}{8\pi}\iint_S \Delta C_{pu}(\xi,\eta)\frac{\partial}{\partial\zeta}\int_{(-x_0+MR)/\beta^2}^{\infty} \times \frac{\exp[-i\omega(\tau_1+x_0)/V]}{r}\,d\tau_1\,d\xi\,d\eta \tag{9}$$

For convenience, let

$$J=\int_{u_1r_1}^{\infty}\frac{\exp[-i\omega(\tau_1+x_0)/V]}{(\tau_1^2+r_1^2)^{1/2}}\,d\tau_1 \tag{10}$$

$$u_1r_1=(-x_0+MR)/\beta^2, \quad r_1^2=y_0^2+z_0^2 \tag{11}$$

It is seen that J depends on ζ only through r_1. It follows that

$$\frac{\partial J}{\partial\zeta}=\frac{\partial J}{\partial r_1}\frac{\partial r_1}{\partial\zeta}=-\frac{z_0}{r_1}\left\{-r_1\int_{u_1r_1}^{\infty}\frac{\exp[-i\omega(\tau_1+x_0)/V]}{(\tau_1^2+r_1^2)^{3/2}}\,d\tau_1 - \frac{M}{R}\frac{\exp[-i\omega(u_1r_1+x_0)/V]}{(1+u_1^2)^{1/2}}\right\} \tag{12}$$

The integral in Eq. (12) can be integrated by parts with the integrated part to be combined with the last term in Eq. (12). After simplification and substitution into Eq. (9), the amplitude of the velocity potential becomes

$$\phi(x,y,z) = \frac{1}{8\pi}\iint_S \Delta C_{pu}(\xi,\eta)\left\{\left(\frac{1}{r_1^2}+\frac{x_0}{Rr_1^2}\right)z_0 \times\exp[-i\omega(u_1r_1+x_0)/V] - i\frac{\omega}{V}\frac{z_0}{r_1} \times\exp(-i\omega x_0/V)\int_{u_1}^{\infty}\left(1-\frac{\lambda}{(1+\lambda^2)^{1/2}}\right) \times\exp(-i\omega r_1\lambda/V)\,d\lambda\right\}d\xi\,d\eta \tag{13}$$

Equation (13) is a convenient form in that the familiar steady expression is immediately recovered when $\omega=0$.

To satisfy the wing boundary condition Eq. (3), the normal wash $w=\partial\phi/\partial z$ must be obtained. For this purpose, Eq. (13) will be approximated through the following discretization. It is assumed that ΔC_{pu} is stepwise constant in the spanwise direction and continuous in the chordwise direction. The resulting chordwise integral will be reduced to finite sums through the midpoint trapezoidal rule according to the QVLM procedure of Ref. 11. For swept planforms, it is more convenient to assume ΔC_{pu} to be stepwise constant in the direction of constant percent chord lines. Therefore, the planform will now be divided into strips in which ΔC_{pu} is taken to be constant along the straight line L joining (x_1,y_1) and (x_2,y_2) where the point with subscript 1 is on the left side of a given strip and 2 is on the right side; see Fig. 1. By fac-

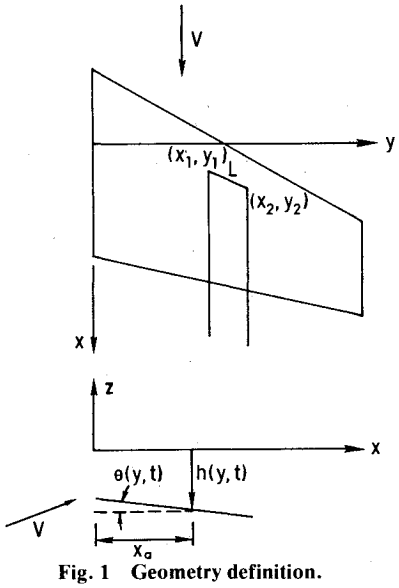

Fig. 1 Geometry definition.

toring ΔC_{pu} out of the spanwise integral, the resulting integrand in the spanwise integration can be integrated by parts. For this purpose, let

$$x_0 = x - \xi = x - x_1 - \tau(x_2 - x_1) \tag{14}$$

$$y_0 = y - \eta = y - y_1 - \tau(y_2 - y_1) \tag{15}$$

The straight line L is now defined by (0,1) in τ. If ϕ_1 is defined to be

$$\phi_1(x,y,z) = \frac{1}{8\pi}\int_L \left(\frac{1}{r_1^2} + \frac{x_0}{Rr_1^2}\right) z_0 \times \exp[-i\omega(u_1 r_1 + x_0)/V]\,d\eta \tag{16}$$

then Eq. (16) can be integrated by parts to give

$$\phi_1(x,y,z) = \frac{1}{8\pi}\left\{F\exp(-i\omega(u_1 r_1 + x_0)/V)\,\Big|_L - \int_L F(-i\omega/V)\frac{\partial}{\partial\eta}(u_1 r_1 + x_0)\exp[-i\omega(u_1 r_1 + x_0)/V]\,d\eta\right\} \tag{17}$$

where

$$F = \int z_0\left(\frac{1}{r_1^2} + \frac{x_0}{Rr_1^2}\right)d\eta = -\tan^{-1}\frac{Qv - (x_2 - x_1)z^2}{z(y_2 - y_1)(A\tau^2 + B\tau + C)^{1/2}} + \tan^{-1}\frac{2a\tau + b}{2(y_2 - y_1)z} \tag{18}$$

$$v = (y_2 - y_1)\tau - (y - y_1) = \eta - y$$

$$a = (y_2 - y_1)^2, \quad b = -2(y - y_1)(y_2 - y_1)$$

$$Q = (x_2 - x_1)(y - y_1) - (x - x_1)(y_2 - y_1)$$

$$A = (x_2 - x_1)^2 + \beta^2(y_2 - y_1)$$

$$B = -2[(x - x_1)(x_2 - x_1) + \beta^2(y - y_1)(y_2 - y_1)]$$

$$C = (x - x_1)^2 + \beta^2(y - y_1)^2 + \beta^2 z^2 \tag{19}$$

A similar procedure can be applied to the second integral (to be denoted by ϕ_2) in Eq. (13). Let

$$I(x,y,z,\xi,\eta) = r_1\int_{u_1}^{\infty}\left(1 - \frac{\lambda}{(1+\lambda^2)^{1/2}}\right)\exp[-i\omega(r_1\lambda + x_0)/V]\,d\lambda \tag{20a}$$

$$= \int_{u_1 r_1}^{\infty}\left(1 - \frac{\tau_1}{(\tau_1^2 + r_1^2)^{1/2}}\right)\exp[-i\omega(\tau_1 + x_0)/V]\,d\tau_1 \tag{20b}$$

It follows that

$$\phi_2(x,y,z) = -i\frac{\omega}{V}\frac{1}{8\pi}\int_L \frac{z}{r_1^2} I(x,y,z,\xi,\eta)\,d\eta = -i\frac{\omega}{V}\frac{1}{8\pi}\left\{\tan^{-1}\frac{2a\tau + b}{2(y_2 - y_1)z} I\,\Big|_L - \int_L \tan^{-1}\frac{2a\tau + b}{2(y_2 - y_1)z}\frac{\partial I}{\partial\eta}\,d\eta\right\} \tag{21}$$

Substituting Eqs. (17) and (21) into Eq. (13) and differentiating with respect to z, it is obtained that

$$\frac{\partial\phi}{\partial z}(x,y,z) = \sum\int_{x_l}^{x_t}\Delta C_{pu}(\xi)\left(\frac{\partial\phi_1}{\partial z} + \frac{\partial\phi_2}{\partial z}\right)d\xi \tag{22}$$

where Σ denotes the summation over all spanwise strips and x_l and x_t are the x coordinates of the leading and trailing edges, respectively, of the chord through the collocation (or control) points (to be specified later). The detailed expressions for $\partial\phi_1/\partial z$ and $\partial\phi_2/\partial z$ are given in Appendix A of Ref. 13. It should be remarked that the steady version of Eq. (22) can be shown to be the result for conventional horseshoe vortices derived by the Biot-Savart law.

With the transformation

$$\xi = x_l + c(1 - \cos\theta)/2 \tag{23}$$

Eq. (22) becomes

$$\frac{\partial\phi}{\partial z}(x,y,z) = \sum\frac{c}{2}\int_0^{\pi}\Delta C_{pu}(\theta)\sin\theta\left(\frac{\partial\phi_1}{\partial z} + \frac{\partial\phi_2}{\partial z}\right)d\theta \tag{24}$$

Note that $\sin\theta$ cancels the square root singularities of ΔC_{pu} at the leading and trailing edges. Therefore, the integral in Eq. (24) can be reduced to a finite sum through the midpoint trapezoidal rule with excellent accuracy. Any Cauchy singularity in the chordwise integral (see Appendix B of Ref. 13) can be accounted for by choosing a special set of control points to be given later. Hence,

$$\frac{\partial\phi}{\partial z}(x,y,z) = \sum\frac{c}{2}\frac{\pi}{N_c}\sum_{k=1}^{N_c}\Delta C_{pu}(\theta_k)\sin\theta_k\left(\frac{\partial\phi_{1k}}{\partial z} + \frac{\partial\phi_{2k}}{\partial z}\right) \tag{25}$$

where N_c is the number of integration points and $\theta_k = (2k-1)\pi/(2N_c)$. Using Eq. (23), it can be determined[11] that the chordwise locations of the "bounded" element of the horseshoe vortices are given by

$$\xi_k = x_l + (c/2)[1 - \cos(2k-1)\pi/2N_c], \quad k = 1,\ldots,N_c \tag{26}$$

The x coordinates of endpoints of the bounded elements are given by

$$x_{1k} = \xi_{1k}, \quad x_{2k} = \xi_{2k} \tag{27}$$

where ξ_{1k} and ξ_{2k} are with x_{ℓ_1}, c_1 and x_{ℓ_2}, c_2 respectively. According to Ref. 11, the control points at which Eq. (3) is to be satisfied must be chosen so that

$$x_i = x_\ell + c[1-\cos(i\pi/N_c)]/2, \quad i=1,\ldots,N_c \tag{28}$$

$$y_j = (b/2)\{1-\cos[j\pi/(N_s+1)]\}/2, \quad j=1,\ldots,N_s \tag{29}$$

where N_s is the number of spanwise strips. The spanwise division of the planform into strips is also based on the cosine distribution

$$y_k = (b/2)\{1-\cos[(2k-1)\pi/2(N_s+1)]\}, \quad k=1,\ldots,N_s+1 \tag{30}$$

Combining Eqs. (3) and (22) and satisfying the boundary condition at the control points, a finite number of ΔC_{pu} values can be computed. These ΔC_{pu} values are then used to obtain the lift and pitching moment coefficients through integration (see Ref. 11).

The calculation of the unsteady leading-edge thrust coefficient is described in Appendix B of Ref. 13. On the other hand, the unsteady side-edge suction is calculated by directly extending the method of steady version in Ref. 14.

The Unsteady Suction Analogy

It is well-known that Polhamus' method of suction analogy in steady flow[8] serves as a simple means for accurate prediction of C_L, C_D, and C_m for wings with the leading-edge vortex flow. The method has also been extended to wings with the vortex-separated flow around the side edges[15] and with the augmented vortex lift.[16] Boyden[21] applied the method to the prediction of steady roll damping derivatives. Since the steady flow can be regarded as a limiting case of the unsteady flow when the reduced frequency k approaches zero, it seems natural to assume that a method of the unsteady suction analogy can be established.

Experiment indicated that the vortex flow on a slender wing under unsteady motion would not achieve its steady-state position and strength instantaneously.[5] Instead, a lag exists relative to the wing motion. This is the so-called "vortex lag." To gain some idea on the effect of reduced frequencies on the vortex lag, the unsteady QVLM was employed to calculate the unsteady leading-edge suction which was then directly taken to be the vortex lift component according to the method of suction analogy. That is, the vortex lag is neglected. The results of roll damping derivatives for a gothic wing are presented in Fig. 2 as a dashed line. It is seen that the direct application of suction analogy (i.e., without vortex lag) overpredicts the roll damping derivative except at very low and high frequencies. This implies that at high frequencies the vortex lag becomes less significant. It should be noted that the conventional aerodynamic lag due to shed vortices being convected at a finite speed ($\simeq V$) and disturbances created at any point being propagated at a speed equal to the ambient speed of sound, has been properly accounted for in the unsteady QVLM. This is illustrated in Fig. 3. On the other hand, the vortex flow component is apparently very much affected by the vortex lag which creates a phase lag between the wing motion and its leading-edge vortex strength buildup at a given station. This vortex lag effect will be the main subject of the following development.

It is assumed that the vortex strength at any given station is mainly affected in the following two ways:

1) It is affected by the vorticity generated upstream and convected downstream. This may be called the "convective effect."

2) It is also affected by the local velocity generated by the wing motion. This may be called the "local effect."

These two effects are discussed below. The main objective is to develop an expression for the phase lag such that at low

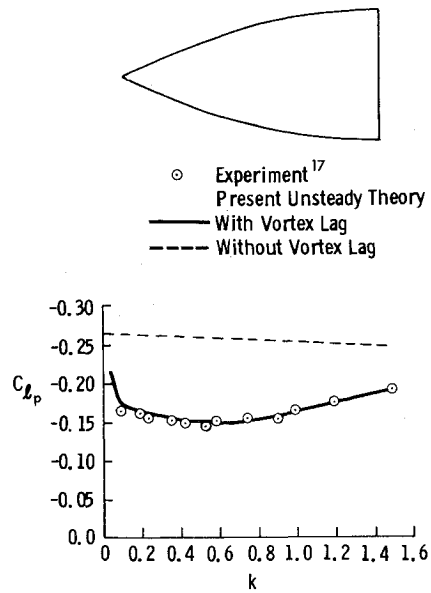

Fig. 2 Effect of reduced frequency on roll damping derivatives for a gothic wing of $A = 0.75$ at $\alpha = 15$ deg (k is based on semispan).

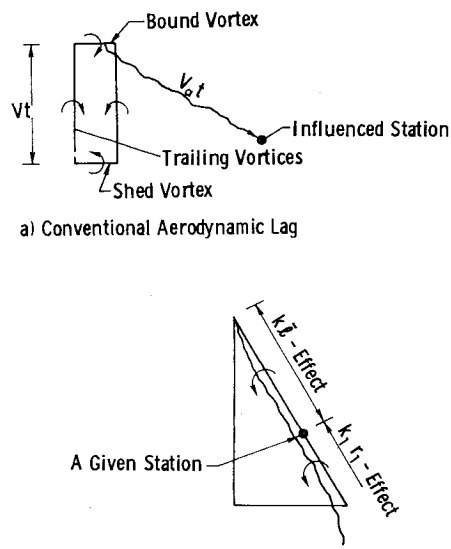

Fig. 3 Illustration of aerodynamic lag mechanisms.

frequencies it increases with frequency, but decreases at high frequencies.

Convective Effect

To develop an expression for the phase lag angle due to this effect, let ℓ be the leading-edge length along which a disturbance has traversed. If the vortex core is assumed to incline at an angle of α_s to the chord plane, then the total length traversed is $\ell/\cos\alpha_s$. The convective speed is assumed to be the freestream component on the chord plane, $V\cos\alpha_s$. Thus, the time taken to traverse a distance equal to $\ell/\cos\alpha_s$ is

$$\text{traversing time} = \ell/V\cos^2\alpha_s$$

If T is the oscillation period, then the above traversing time is equivalent to

$$\phi_1 = \frac{\ell}{V(\cos^2\alpha_s)T} = \frac{\omega\ell_r}{V}\frac{\ell}{\ell_r\cos^2\alpha_s(2\pi)}, \quad \text{cycles} \tag{31}$$

In radians, it is

$$\phi_l = k\ell/\ell_r \cos^2\alpha_s, \quad k = \omega\ell_r/V \tag{32}$$

Equation (32) represents the contribution of direct convective effect to the vortex lag. This phase lag should be increased by the effect of shed vortices trailing behind (called trailing vortices in the following). The simplest way to represent this latter effect is to use the result of classical airfoil theory in oscillatory motion. According to Ref. 18, the phase lag of aerodynamic characteristics due to trailing vortices can be obtained from Theodorsen's circulation function

$$C(k) = F(k) + iG(k) \tag{33}$$

The reduced frequency k in Eq. (33) is based on half chord which is taken as unity. The ratio $|G(k)|/F(k)$ is indicative of phase lag of aerodynamic forces relative to the motion because of trailing vortices. It varies from a maximum of 0.2697 at $k = 0.30$ to 0 at both $k = 0$ and ∞. To make this ratio applicable in the present three-dimensional application, it should be noted that for a unit reference length traversed [i.e., $\ell = 1.0$ in Eq. (32)], and with $\ell_r = 1.0$ and $\alpha_s = 0$ [i.e., the conditions usually associated with Eq. (33)], Eq. (32) shows that the phase lag angle is equal to the reduced frequency. Therefore, in the present application, it is assumed that for a unit length traversed, the additional phase lag due to trailing vortices is equivalent to increasing the reduced frequency by an amount equal to

$$k_l = |G(k')|/F(k') \tag{34}$$

where k' is based on half root chord, i.e.,

$$k' = kc_r/2\ell_r \tag{35}$$

Therefore, an equivalent reduced frequency k_e can be defined as

$$k_e = k + k_l \tag{36}$$

Equation (32) is now modified as

$$\phi_2 = k_e\ell/\ell_r \cos^2\alpha_s \tag{37}$$

To determine the upstream extent of disturbances which can affect a given point on the leading edge by convection, it is noted that if $\phi_2 \geq \pi/2$, a disturbance from the upstream end cannot reach that point before the upstream condition is changed in an oscillatory motion. Therefore, a characteristic length ℓ_c may be defined as the length ℓ in which $\phi_2 = \pi/2$ is achieved with $\alpha_s = 0$. Using this condition in Eq. (37) and solving ℓ ($= \ell_c$), it is obtained that

$$\ell_c = \pi\ell_r/2k_e \tag{38}$$

As k_e is increased, ℓ_c is reduced so that it may be less than the distance from a given station to the wing apex. Therefore, the actual upstream extent of vortex core affecting a given point is the lesser of ℓ_c and the upstream leading-edge length to the apex ℓ. This extent is denoted by L.

Lumped Phase Angle. Equation (37) gives the phase lag contributed by an individual disturbance. In Ref. 3, Eq. (32) (without the $\cos^2\alpha_s$ factor) was used as the lumped phase angle for the overall effect. In the present method, this idea of using the lumped phase angle will be modified as follows. The direct convective effect is accounted for by using a mean traversing distance $\bar{\ell}$ weighted with respect to $c_s c$, where c_s is the magnitude of the sectional unsteady leading-edge suction coefficient and c the local chord. The value of $c_s c$ represents the sectional vortex lift due to the oscillatory wing motion in the present method of unsteady suction analogy. Furthermore, if ℓ_c is less than the total leading-edge length upstream of a given station ℓ, the trailing vortex effect is assumed to be reduced by a factor ℓ_c/d, where d is the total leading-edge length. This is because k_l is used without modification only if upstream full length of the vortex core participates in producing the phase lag. Let

$$r_l = \ell_c/d \tag{39}$$

It follows that the convective lumped phase is

$$\phi_c = (k\bar{\ell} + k_l r_l L)/\ell_r \cos^2\alpha_s \tag{40}$$

Physically, Eq. (40) implies that the vorticity generated upstream of a given station affects this station not only while it is still upstream (i.e., the $k\bar{\ell}$ term) but does so continuously while it moves downstream (the $k_l r_l$ term). If the period of oscillation T is short, the trailing wake effect should be diminished (the r_l factor).

The convective effect described above is also illustrated in Fig. 3.

Local Effect

Since the local velocity is generated by the local wing motion almost instantaneously, the phase lag due to this effect can be assumed to be small. This is similar to the quasisteady component in the classical unsteady airfoil theory.[18]

At high frequencies (i.e., small T) the convecting vortices have only a short time to influence a given station before the local condition is changed. This means that the convective effect is less important and the local effect becomes relatively more significant, so that the phase lag is reduced. This behavior of phase lag angle at high reduced frequencies is evident in the test data of Ref. 17 for the roll damping derivatives. This implies that the phase lag angle should be inversely proportional to the reduced frequency at high k.

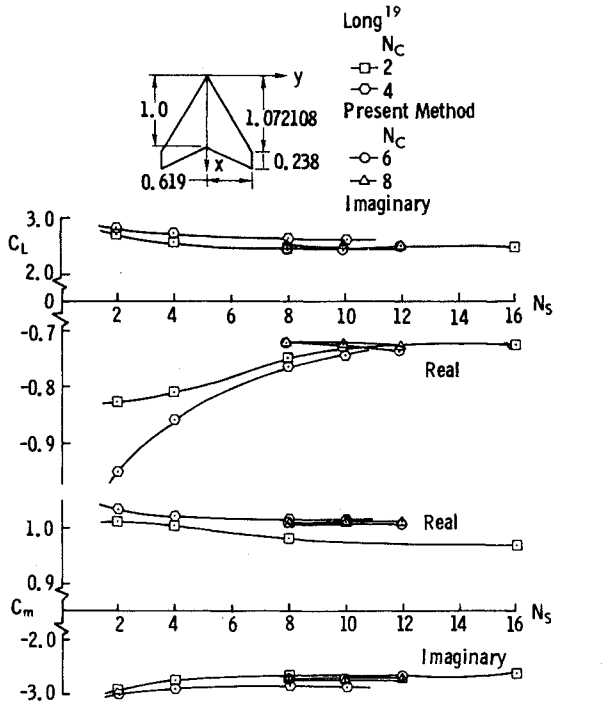

Fig. 4 Aerodynamic characteristics of AGARD E wing of $A = 2.0$ at $M = 0.781$ in plunging oscillation with amplitude = semispan and $k = 1.0$ based on semispan.

To model this "local effect" mathematically, note that ℓ_c given in Eq. (38) possesses the required mathematical property with respect to the reduced frequency. Therefore a localization factor a_c can be defined as

$$a_c = \ell_c/\ell, \quad a_c \leq 1.0 \tag{41}$$

The magnitude of a_c decreases as the reduced frequency is increased. An effective frequency is then defined as the weighted average of the convective equivalent frequency and that due to the local effect given by a_c

$$k_{\text{eff}} = a_c(k\bar{\ell}/L + k_1 r_1) + (1-a_c)a_c \tag{42}$$

and the vortex phase lag angle is defined as

$$\phi_{\text{eff}} = k_{\text{eff}} L/\ell_r \cos^2\alpha_s \tag{43}$$

where L is the lesser of ℓ and ℓ_c. Equations (42) and (43) possess the required properties of phase lag angle in that at low reduced frequencies $a_c = 1.0$ and the convective effect would dominate. On the other hand, at high frequencies a_c is small so that ϕ_{eff} is reduced.

Aerodynamic Characteristics

Once the vortex lag phase angle is obtained, the unsteady leading-edge singularity parameter ($C_u = a + ib$) should be modified to give

$$A = (a+ib)(\cos\phi_{\text{eff}} - i\sin\phi_{\text{eff}}) = A_1 - iA_2 \tag{44}$$

where

$$A_1 = a\cos\phi_{\text{eff}} + b\sin\phi_{\text{eff}} \tag{45}$$

$$A_2 = a\sin\phi_{\text{eff}} - b\cos\phi_{\text{eff}} \tag{46}$$

It follows that the total magnitude of singularity parameter will be (with A_s being the steady part)

$$C_Q = A_s \pm (A_1 - iA_2) \tag{47}$$

and

$$C_Q^2 \cong A_s^2 \pm 2(A_1 - iA_2)A_s \tag{48}$$

where the + sign is for additional positive loading. Hence, the sectional leading-edge thrust coefficient is given by[11]

$$c_t = \pi C_Q^2 (1 - M^2\cos^2\Lambda_\ell)^{1/2}/(2\cos\Lambda_\ell) \tag{49}$$

Similar procedures are also applicable to the calculation of side-edge suction.

Note that the calculated lifting pressure coefficients for steady flow (ΔC_{ps}) and unsteady flow (ΔC_{pu}) are equal to two times the corresponding vortex densities in the linear theory. They are assumed to interact with the freestream velocity component in the chord plane to produce the normal force[8]

$$\Delta C_N = (\Delta C_{ps} + \Delta C_{pu})\cos(\alpha_s + \Delta\alpha) \simeq \Delta C_{ps}\cos\alpha_s - \Delta\alpha\Delta C_{ps}\sin\alpha_s + \Delta C_{pu}\cos\alpha_s \tag{50}$$

The normal force is then used to determine the aerodynamic characteristics in a way similar to the steady flow case. The details can be found in Ref. 11 and will not be repeated here.

Results and Discussions

Some attached flow results by the present method in incompressible flow have been reported in Refs. 9 and 10. Some additional attached flow results for a swept wing in plunging oscillation at $M = 0.781$ are compared in Fig. 4 with those obtained by a kernel function method.[19] It is seen that the present method has good convergence characteristics with respect to the numbers of chordwise elements (N_c) and spanwise strip (N_s) used. Similarly convergent results for the unsteady leading-edge suction (not shown) have also been obtained.

Roll Damping Derivatives

The prediction of roll damping derivatives for a gothic wing illustrated earlier in Fig. 2 is further presented in Fig. 5 with various approximations. As shown therein, the attached flow method is definitely inadequate. On the other hand, an appropriate vortex lag model is needed for good prediction. If only the convective effect given by Eq. (40) is incorporated in the method, the results will be accurate only at low reduced frequencies.

It is a well-known experimental fact that slender wings tend to exhibit wing rocking at high angles of attack.[20] One possible reason for this is the reduction of roll damping at high angles of attack. This is illustrated in Fig. 6. Similar trend of variation of C_{l_p} with α is also shown for a delta wing of $A = 1.147$ ($\Lambda = 74$ deg)[21] in Fig. 7 and for HP115 aircraft[22] in Fig. 8. It is clearly indicated in Fig. 7 that even at a small reduced frequency of 0.2, the steady flow method is not accurate at high angles of attack. It is also seen that the vortex lag effect is very significant.

Longitudinal Dynamic Stability Derivatives

In general, the amplitudes of lift and pitching moment coefficients in oscillatory motion can be expressed in terms of stability derivatives as follows[23]

$$C_N = ik\frac{h}{\ell_r}C_{N_{\dot{h}}} - k^2 C_{N_{\ddot{h}}}\frac{h}{\ell_r} + \theta C_{N_\theta} + ik\theta C_{N_{\dot{\theta}}} + \ldots \tag{51}$$

$$C_m = ik\frac{h}{\ell_r}C_{m_{\dot{h}}} - k^2 C_{m_{\ddot{h}}}\frac{h}{\ell_r} + \theta C_{m_\theta} + ik\theta C_{m_{\dot{\theta}}} + \ldots \tag{52}$$

At zero frequency, $C_{m_\theta} = C_{m_\alpha}$ and at very small frequencies,

$$C_{m_{\dot{\theta}}} = C_{m_q} + C_{m_{\dot{\alpha}}} \tag{53}$$

where $C_{m_{\dot{\alpha}}}$ can be shown to be equal to $C_{m_{\dot{h}}}$.

In the present method, the vortex lag concept applies only to those loadings associated with time rate of change of atti-

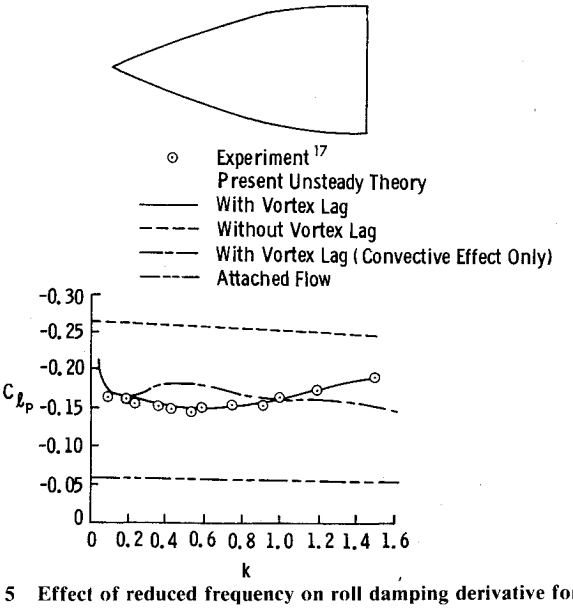

Fig. 5 Effect of reduced frequency on roll damping derivative for a gothic wing of $A = 0.75$ at $\alpha = 15$ deg (k is based on semispan).

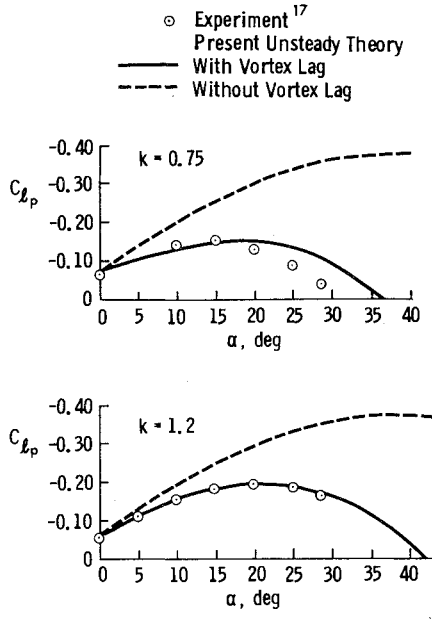

Fig. 6 Effect of angle of attack on roll damping derivative of a gothic wing of $A = 0.75$.

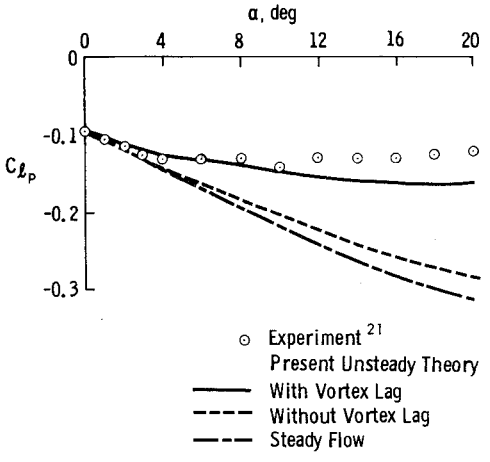

Fig. 7 Effect of angle of attack on roll damping derivatives for a delta wing of $A = 1.147$, $k = 0.12$ for $\alpha \leq 4$ deg and $k = 0.2$ for $\alpha > 4$ deg (k is based on semispan).

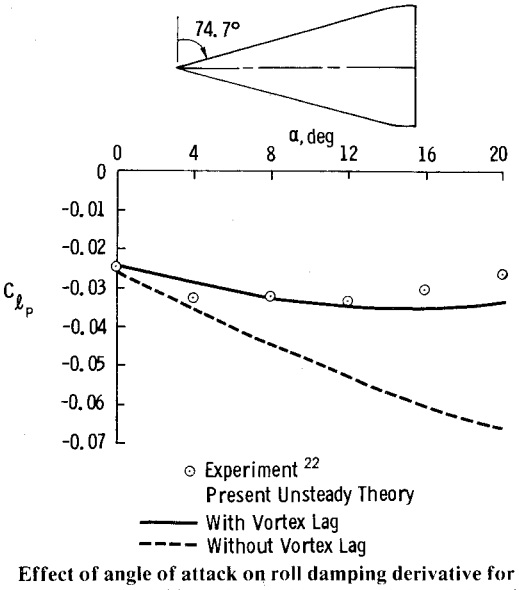

Fig. 8 Effect of angle of attack on roll damping derivative for British HP 115 aircraft, $A = 0.925$, wing incidence angle = 1.5 deg ($k = 1.42$ based on root chord).

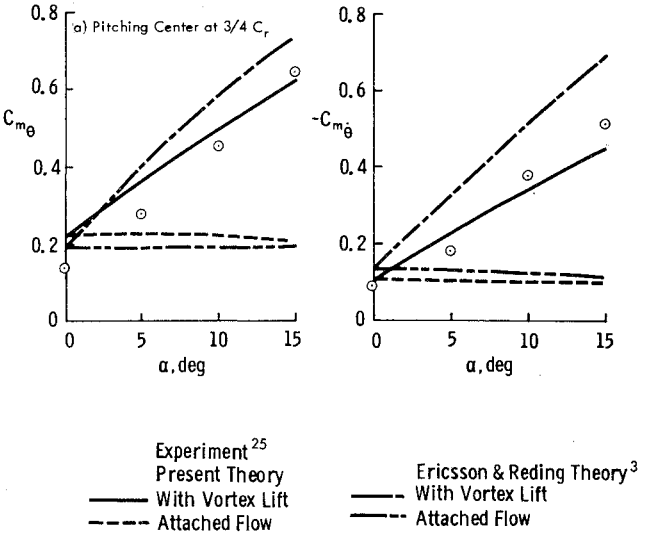

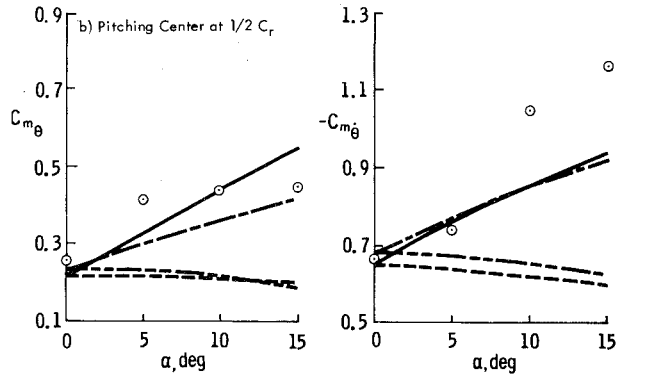

Fig. 9 Pitching derivatives for a delta wing of $A = 0.654$ at $M = 0$ and $k = 0.21$ based on half root chord.

tudes [such as $\dot{h}, \dot{\theta}, \dot{\phi}_r(t)$ in Eq. (1b)]. In addition, it is applied only to the vortex flow with increasing vortex strength due to the motion. This is based on the experimental observation that the extra lift due to an upgust takes some time to build up, whereas it vanishes quickly when the wing returns to undisturbed air.[24] According to some unpublished calculations by the present method, this behavior can be explained by the presence and absence of vortex lag, respectively.

Results for pitching derivatives for a delta wing of $A = 0.654$ ($\Lambda = 80.71$ deg) at $M = 0$ and $k = 0.21$ are compared with data[25] and Ericsson and Reding's theory[3] in Fig. 9. It is seen from Fig. 9 that the present method appears at least as accurate as the method of Ref. 3. The pitching derivatives for an ogee wing at $k = 1.0$ are presented in Fig. 10 and the plunging derivatives for the same wing at $k = 2.7$ based on root chord are shown in Fig. 11. At such high frequencies, no other theoretical results are available for comparison. The present vortex flow results are in reasonable agreement with the data. Note that the data have considerable scatter. In the calculation, a plane wing was assumed, although the experimental model was a cambered one (the camber shape was not defined in Ref. 26). This may have affected somewhat the agreement in the predicted C_{m_θ} with data.

In the present formulation of vortex lag, Theodorsen's circulation function was used as shown in Eq. (34). Strictly speaking, it is valid only in incompressible flow. To indicate the accuracy of the present method in compressible flow, some results at $M = 0.8$ are presented in Fig. 12. The damping derivative is well predicted. The overprediction of C_{m_θ} may be due to the omitted camber effect and the aeroelastic effect at high dynamic pressure (being 206 lb/ft^2 or 9863 Pa).

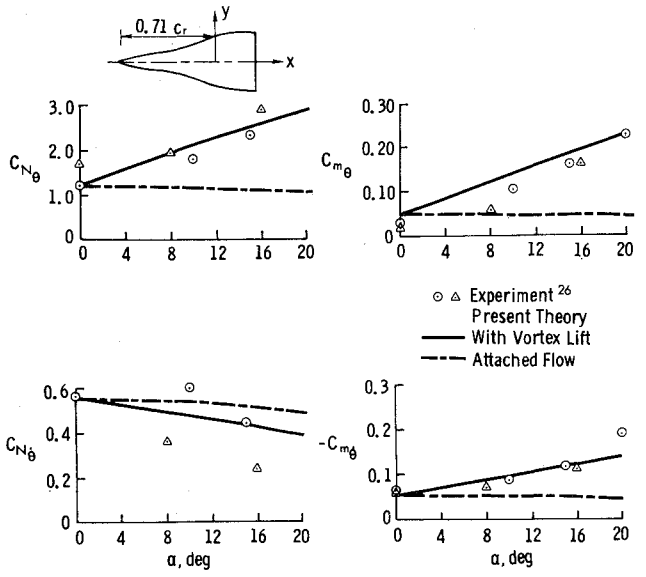

Fig. 10 Pitching derivatives for an ogee wing of $A = 0.924$ at $M = 0$ and $k = 1.0$ based on c_r.

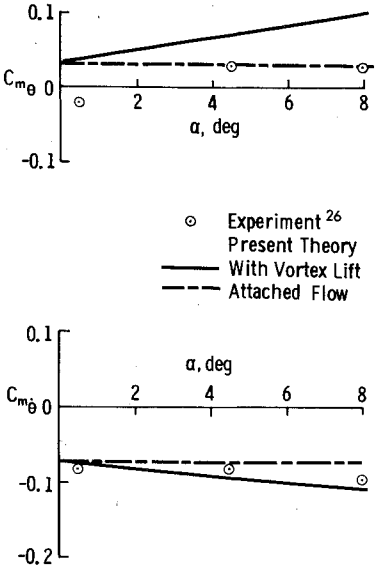

Fig. 12 Plunging derivatives for an ogee wing of $A = 0.925$ at $M = 0.8$ and $k = 0.23$ based on c_r (pitching center at 0.71 c_r from apex).

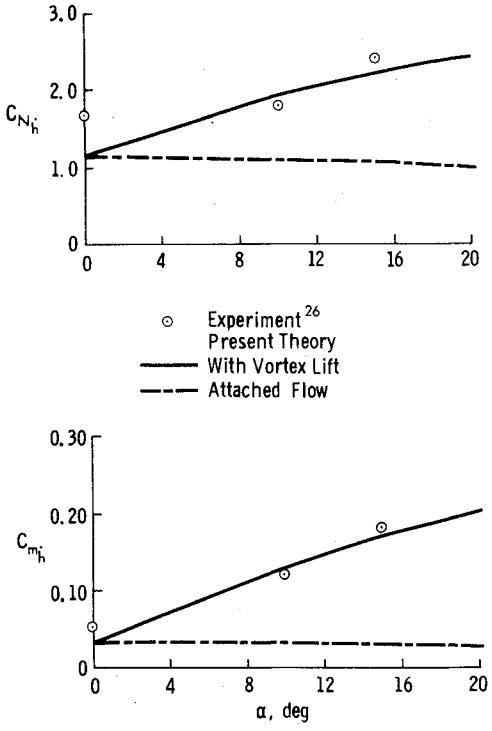

Fig. 11 Plunging derivatives for an ogee wing of $A = 0.924$ at $M = 0$ and $k = 2.7$ based on c_r (moment center at 0.71 c_r from apex).

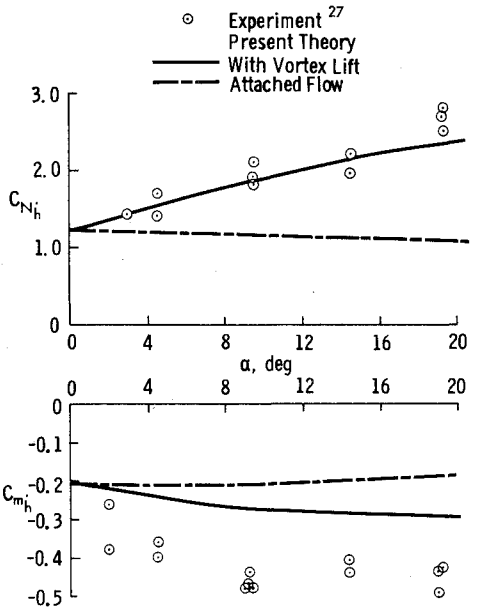

Fig. 13 Plunging derivatives for a delta wing of $A = 1.0$ at $M = 0.2$ and $k = 1.6$ based on $2c_r/3$ (moment center at midroot chord).

Further comparison of predicted plunging derivatives with data[27] for a delta wing of $A = 1.0$ ($\Lambda = 75.96$ deg) at $k = 1.6$ is presented in Fig. 13. The agreement in the normal force derivative is quite good. However, $|C_{m_{\dot h}}|$ is underpredicted. The reason is not known.

For a planform with swept trailing edges or finite tip chord, Lamar[16] developed the concept of augmented vortex lift. It is based on the assumption that the leading-edge vortex, when it passes over an additional planform area in the downstream direction, will induce additional loading proportional to the length it traverses. The importance of this concept is illustrated in Fig. 14 for a cropped delta wing at $k = 1.2$. It is seen that the side-edge vortex lift effect is very significant and the augmented vortex lift helps improve the agreement with data at high angles of attack. Further comparison with other cropped delta wing data[28] is shown in Fig. 15. The agreement in this case is less satisfactory. The test was done at a Reynolds number of 1.5×10^6. Reference 28 indicated that when the Reynolds number was reduced by half, $|C_{m_\theta}|$ was increased by 20% and $|C_{m_{\dot\theta}}|$ was increased by 7%. In other words, if the Reynolds number is increased further from the test value, the magnitude of all derivatives will be reduced so that the agreement with prediction can be improved.

A more complicated configuration to apply the concept of augmented vortex flow is the cropped arrow wing shown in Fig. 16. Two possible values of characteristic length $\bar{c}$ to be used in Lamar's method are also indicated in the figure. With $\bar{c}$ equal to tip chord, the predicted pitch damping agrees well with data.[28] The overprediction of $|C_{m_\theta}|$ with the assumption of sharp edges is most likely the result of overpredicting the edge-separated vortex strength, because the airfoil section on the test model is of 10% thickness ratio with rounded leading edge. Corrections with Kulfan's method[29] appear to produce good agreement with the data.

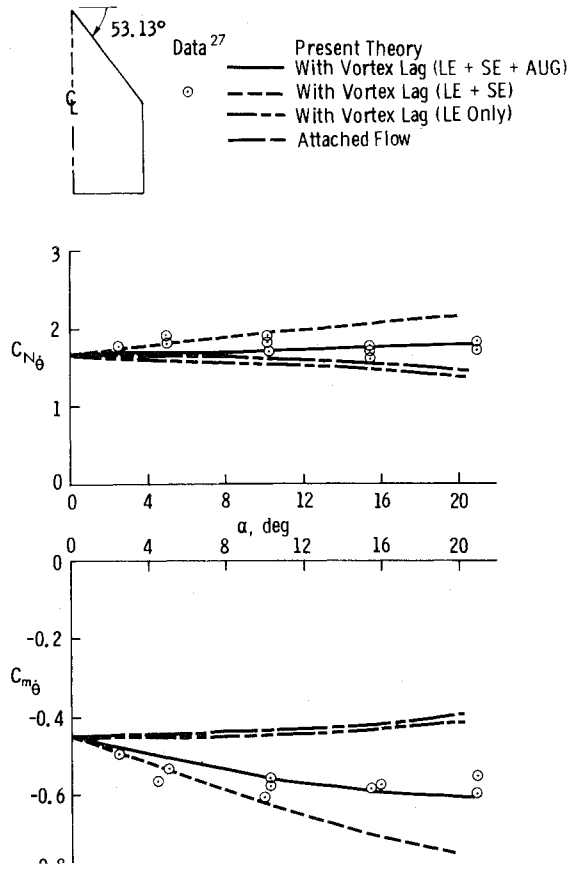

Fig. 14 Pitching derivatives for a cropped delta wing of $A = 1.0$ and $\lambda = 0.5$ at $M = 0$ and $k = 1.2$ based on $\bar{c}$ (pitching center at $\bar{c}/4$).

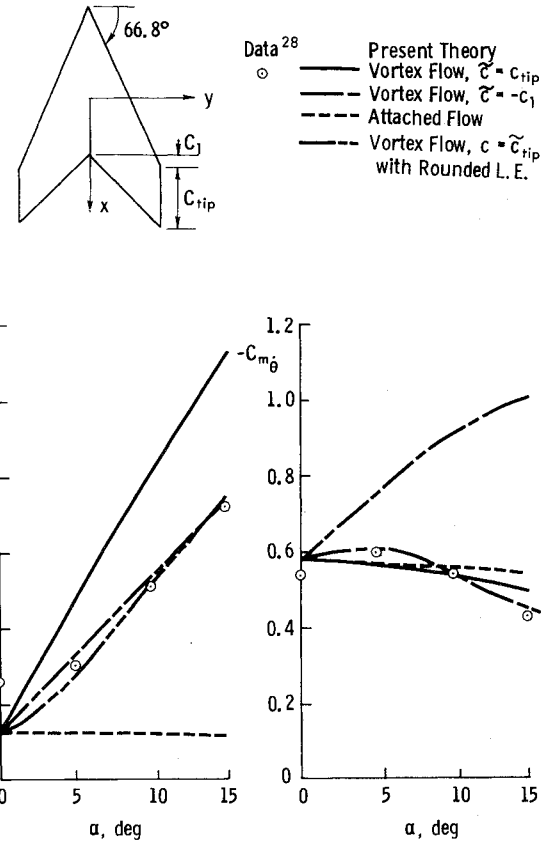

Fig. 16 Pitching derivatives for a cropped arrow wing of $A = 1.32$ and $\lambda = 0.39$ at $M = 0$ and $k = 0.3$ based on average chord (pitching center at 0.883 of average chord).

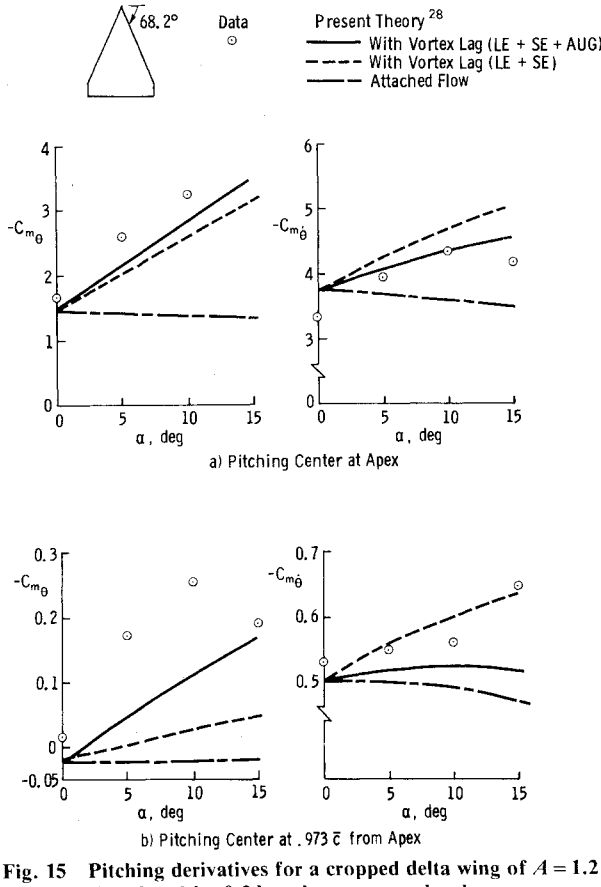

Fig. 15 Pitching derivatives for a cropped delta wing of $A = 1.2$ and $\lambda = 1/7$ at $M = 0$ and $k = 0.3$ based on average chord.

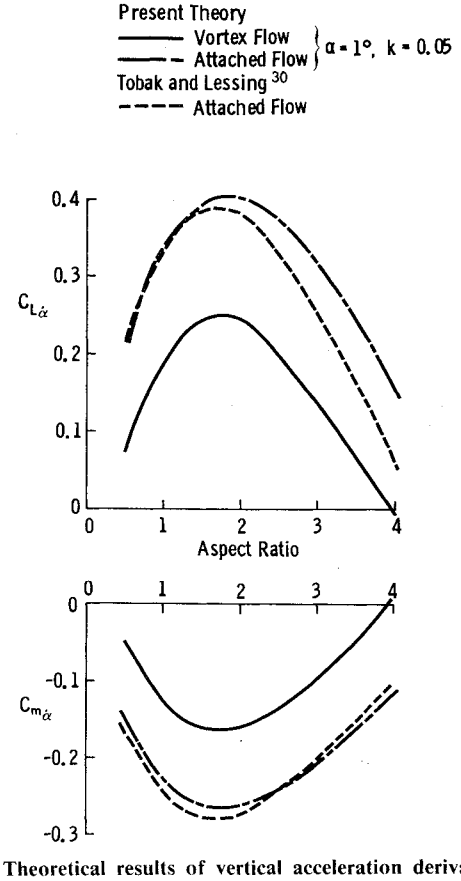

Fig. 17 Theoretical results of vertical acceleration derivatives for delta wings at $M = 0$ (moment center at apex).

The existing method in the USAF Stability and Control Datcom for predicting $C_{L_{\dot{\alpha}}}$ and $C_{m_{\dot{\alpha}}}$ is based on Tobak and Lessing's theory[30] for delta wings in attached flow. The present results in attached flow are compared with those from Ref. 30 in Fig. 17. The agreement is seen to be good. On the other hand, the vortex flow tends to reduce the magnitude of $C_{L_{\dot{\alpha}}}$ and $C_{m_{\dot{\alpha}}}$ because of vortex lag effect.

Conclusions

A method of the unsteady suction analogy has been developed. The method is applicable to any reduced frequency. Extensive comparison with data indicated that damping derivatives, including roll and pitch damping, can be accurately predicted by the present method. On the other hand, the agreement of predicted pitch stiffness derivatives with the data depends on the Reynolds number, possible aeroelastic effect, and the degree of edge-separated vortex flow on the model. On the average, fair agreement has been obtained.

Acknowledgment

This research was supported by NASA Grant NAG-1-75 through Langley Research Center.

References

[1] "Dynamic Stability Parameters," AGARD CP-235, May 1978.

[2] Randall, D.G., "Oscillating Slender Wings in the Presence of Leading-Edge Separation," British RAE Structures Rept. 286, 1963.

[3] Ericsson, L.E. and Reding, J.P., "Unsteady Aerodynamics of Slender Delta Wings at Large Angles of Attack," *Journal of Aircraft,* Vol. 12, Sept. 1975, pp. 721-729.

[4] Ericsson, L.E. and Reding, J.P., "Effect of Angle of Attack and Mach Number on Slender-Wing Unsteady Aerodynamics," *Journal of Aircraft,* Vol. 15, June 1978, pp. 358-365.

[5] Lambourne, N.C., Bryer, D.W., and Maybrey, J.F.M., "The Behavior of the Leading-Edge Vortices over a Delta Wing Following a Sudden Change of Incidence," British Aeronautical Research Council, R&M No. 3645, 1969.

[6] Atta, E.H., Kandil, O.A., Mook, D.T., and Nayfeh, A.H., "Unsteady Aerodynamic Loads on Arbitrary Wings Including Wing-Tip and Leading-Edge Separation," AIAA Paper 77-156, 1977.

[7] Schneider, C.P., "Analytical Determination of Dynamic Stability Parameters," *Dynamic Stability Parameters,* AGARD Lecture Series Preprint LSP-114, Feb. 1981, Paper 12.

[8] Polhamus, E.C., "Prediction of Vortex-Lift Characteristics by a Leading-Edge Suction Analogy," *Journal of Aircraft,* Vol. 8, April 1971, pp. 193-199.

[9] Lan, C.E., "The Unsteady Quasi-Vortex-Lattice Method with Applications to Animal Propulsion," *Journal of Fluid Mechanics,* Vol. 93, Pt. 4, 1979, p. 747.

[10] Lan, C.E., "Some Applications of the Quasi-Vortex-Lattice Method in Steady and Unsteady Aerodynamics," *Vortex Lattice Utilization,* NASA SP-405, 1976, Paper 21.

[11] Lan, C.E., "A Quasi-Vortex-Lattice Method in Thin Wing Theory," *Journal of Aircraft,* Vol. 11, Sept. 1974, pp. 518-527.

[12] Richardson, J.R., "A Method for Calculating the Lifting Forces on Wings (Unsteady Subsonic and Supersonic Lifting-Surface Theory)," British Aeronautical Research Council, R&M No. 3157, April 1955.

[13] Lan, C.E., "The Unsteady Suction Analogy and Applications," AIAA Paper 81-1875, Aug. 1981.

[14] Lan, C.E., "Calculation of Lateral-Directional Stability Derivatives for Wing-Body Combinations with and without Jet-Interaction Effects," NASA CR-145251, 1977.

[15] Lamar, J.E., "Extension of Leading-Edge-Suction Analogy to Wings with Separated Flow Around the Side Edges at Subsonic Speeds," NASA TR R-428, Oct. 1974.

[16] Lamar, J.E., "Recent Studies of Subsonic Vortex Lift Including Parameters Affecting Stable Leading-Edge Vortex Flow," *Journal of Aircraft,* Vol. 14, Dec. 1977, pp. 1205-1211.

[17] Owen, T.B., "Low-Speed Wind Tunnel Measurements of Oscillatory Rolling Derivatives on a Sharp-Edged Slender Wing: Effects of Frequency Parameter and of Ground," British Aeronautical Research Council, R&M No. 3617, 1968.

[18] von Kármán, Th. and Sears, W.R., "Airfoil Theory for Non-Uniform Motion," *Journal of the Aeronautical Sciences,* Vol. 5, Aug. 1938, pp. 379-390.

[19] Long, G., "An Improved Method for Calculating Generalized Airforces on Oscillating Wings in Subsonic Flow," British Aeronautical Research Council, R&M No. 3657, 1969.

[20] Chambers, J.R., Gilbert, W.P., and Nguyen, L.T., "Results of Piloted Simulator Studies of Fighter Aircraft at High Angles of Attack," *Dynamic Stability Parameters,* AGARD CP-235, May 1978, Paper 33.

[21] Boyden, R.P., "Effects of Leading-Edge Vortex Flow on the Roll Damping of Slender Wings," *Journal of Aircraft,* Vol. 8, July 1971, pp. 543-547.

[22] Thompson, J.S., Fail, R.A., and Inglesby, J.V., "Low-Speed Wind-Tunnel Measurements of the Oscillatory Lateral Stability Derivatives for a Model of Slender Aircraft (HP 115) Including the Effects of Frequency Parameter," British Aeronautical Research Council, Current Papers No. 1097, 1970.

[23] Rodden, W.P. and Giesing, J.P., "Application of Oscillatory Aerodynamic Theory to Estimation of Dynamic Stability Derivatives," *Journal of Aircraft,* Vol. 7, May-June 1970, pp. 272-275.

[24] Roberts, D.R. and Hunt, G.K., "Further Measurements of Transient Pressures on a Narrow-Delta Wing due to a Vertical Gust," British Aeronautical Research Council, Current Papers No. 1012, 1966.

[25] Woodgate, L., "Measurements of the Oscillatory Pitching-Moment Derivatives on a Series of Three Delta Wings in Incompressible Flow," British Aeronautical Research Council, R&M No. 3628, 1968.

[26] Thompson, J.S. and Fail, R.A., "Oscillatory-Derivative Measurements on Sting-Mounted Wind Tunnel Models: Method of Test and Results for Pitch and Yaw on a Cambered Ogee Wing at Mach Numbers up to 2.6," British Aeronautical Research Council, R&M No. 3355, 1962.

[27] Schmidt, E., "Experimentelle und Theoretische Untersuchungen über die Instationären Flugmechanischen Derivativa der Längsbewegung an Schlanken Flugkörpern bei Mässiger Geschwindigkeit," *Jahrbuch 1971 der DGLR,* pp. 71-97.

[28] Scruton, C., Woodgate, L., and Alexander, A.J., "Measurements of the Aerodynamic Derivatives for Swept Wings of Low Aspect Ratio Describing Pitching and Plunging Oscillations in Incompressible Flow," British Aeronautical Research Council, R&M No. 2925, 1953.

[29] Kulfan, R.M., "Wing Airfoil Shape Effects on the Development of Leading-Edge Vortices," AIAA Paper 79-1675, Aug. 1979.

[30] Tobak, M. and Lessing, H.C., "Estimation of Rotary Stability Derivatives at Subsonic Speeds," AGARD Rept. 343, 1961.